

An Efficient, Highly Homogeneous Radiofrequency Coil for Whole-Body NMR Imaging at 1.5 T

CECIL E. HAYES,* WILLIAM A. EDELSTEIN,† JOHN F. SCHENCK,†
OTWARD M. MUELLER,† AND MATTHEW EASH‡

**Applied Science Laboratory, General Electric Company, Medical Systems Business Group, P.O. Box 414, W-875, Milwaukee, Wisconsin 53201; †General Electric Corporate Research & Development Center, Schenectady, New York 12345; and ‡Engineering Department, General Electric Company, Medical Systems Group, Milwaukee, Wisconsin 53201*

Received December 28, 1984; revised March 18, 1985

We have developed radiofrequency coils for high-field head and whole-body imaging which achieve near optimal rf field (B_1) homogeneity and signal-to-noise ratio (SNR). The design, based on a lumped element delay line, has a number of advantages. The rf field uniformity is significantly better than that of a saddle coil or slotted tube resonator. The improved B_1 homogeneity is needed to generate accurate multiecho pulse sequences. Using this coil, we obtain, as expected, the nearly linear increase in signal-to-noise as a function of frequency or static magnetic field B_0 (I). The coil's cylindrical symmetry allows quadrature drive and reception which decreases rf power requirements by a factor of two and increases signal-to-noise by a factor of $\sqrt{2}$ (2). Our head-size coil and body-size coil operate at 64 MHz. Designs for operation at lower frequencies or somewhat higher frequencies are possible. Small scale versions of this coil design should be applicable to conventional NMR spectroscopy.

The use of a superconducting solenoidal magnet for whole-body MR imaging requires a transverse rf field within a cylindrical volume. A perfectly homogeneous transverse magnetic field in an infinitely long cylinder can be produced by a surface current which runs along the length of the cylinder and is proportional to $\sin \theta$, where θ is the cylindrical coordinate azimuthal angle. The conventional saddle coil (3) actually approximates the ideal sinusoidal current distribution for six equally spaced values of θ ($\theta = 0, 60, 120, 180, 240, 300^\circ$). Four conductors carry currents of equal magnitude whereas no conductors are needed at $\theta = 0$ and 180° because the currents there are zero. To improve the approximation to the ideal current distribution with more conductors requires a means of developing unequal, sinusoidally weighted currents in adjacent conductors. A standing wave in a transmission line generates the required sinusoidal current distribution. Hinshaw and Gauss (4) employ this principle by winding a one-wavelength-long coaxial cable onto a toroidal form. They removed the coaxial shielding from the cable lying on the inner diameter of the toroid. The exposed portions of the center conductor of the cable generate a homogeneous rf magnetic field in the inner bore of the toroid. This structure is limited to lower frequencies by the need to wind a many-turn toroid from a single

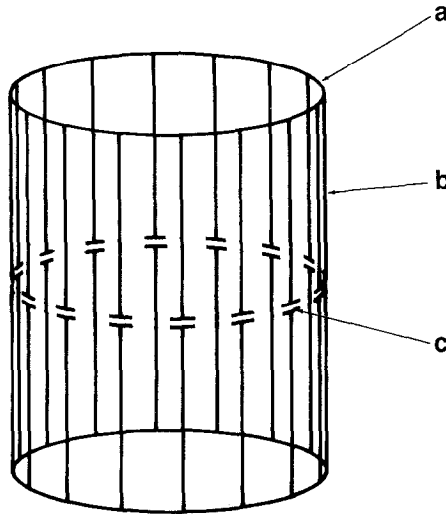


FIG. 1. Low-pass version of a birdcage resonator. (a) Circular end ring; (b) straight segment; (c) capacitor.

wavelength of cable. Roeschmann (5) demonstrated the high-frequency, one-turn limit of this structure at 85 MHz by exposing the center conductor at only two places. His coil has a lower rf field homogeneity similar to that of a saddle coil.

Our design, which we call a “birdcage” resonator, is shown in its low-pass version in Fig. 1. It consists of two circular end rings connected by N equally spaced straight segments, each of which includes a capacitance C . The birdcage resonator can be analyzed using a lumped element balanced delay line (Fig. 2) with ends connected to form a closed loop. All the inductors L_2 , representing the straight segments, are coupled to each other by mutual inductance. Likewise, all of the $\frac{1}{2}L_1$ inductors, representing the individual segments of the end rings, are inductively coupled. The resonant phenomena can be understood by considering wave propagation in a periodic structure (6). Periodic boundary conditions apply to the closed loop. Each of the N repeated elements of the transmission line introduces a phase shift $\Delta\phi(\omega)$.

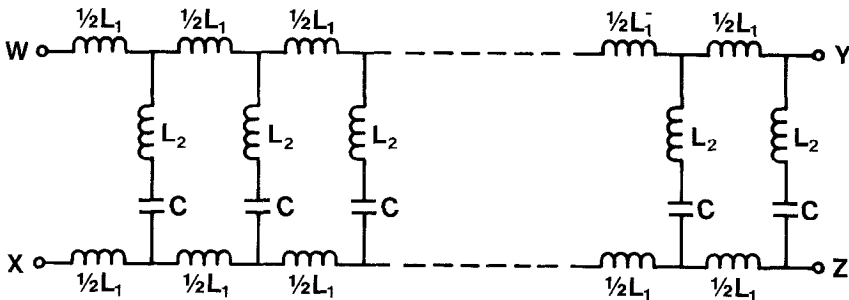


FIG. 2. Lumped element equivalent circuit of a low-pass birdcage. Points w and x connect to points y and z , respectively.

The total phase shift must be an integer multiple of 2π ; hence, the resonant condition is $N\Delta\phi(\omega) = 2\pi M$. A straightforward deviation of $\Delta\phi(\omega)$ is possible if the network is simplified by setting L_2 and all mutual inductances equal to zero. The simplified network is a low-pass filter and has a spectrum with $N/2$ resonances (assuming N is even) at frequencies given by

$$\omega = \frac{2}{\sqrt{L_1 C}} \sin \frac{\pi M}{N} \quad [1]$$

where $1 \leq M \leq N/2$. A standing wave in the low-frequency mode ($M = 1$) generates currents in straight segments proportional to $\sin \theta$ which produce a homogeneous B_1 field inside the cylinder. Higher frequency resonant modes produce increasingly less homogeneous B_1 fields as M increases. For $M = N/2$, adjacent straight segments have currents equal in magnitude but of opposite phase. Setting L_2 to a realistic nonzero value is equivalent to replacing C with $C' = C/(1 - \omega^2 L_2 C)$ in Eq. [1]. Hence L_2 lowers the higher frequency resonant modes disproportionately and causes a compression of the network's spectrum. On the other hand, reintroducing the mutual inductance tends to spread out the spectrum. We have also developed a high-pass version of the birdcage in which the capacitors are spaced around the end rings and the straight segments are the chief inductors.

An alternative interpretation of the low-pass birdcage resonator may provide some intuitive insight. Assume there is a uniform B_1 field along the $\theta = 0$ direction in the cylinder. Consider the closed loop made up of two straight segments located at $+\theta$ and $-\theta$, respectively, and connected by portions of each end ring. The net flux through this closed loop and the associated inductive voltage developed in it are proportional to $2 \sin \theta$. Since the capacitive voltage drops due to the current in the wires at $+\theta$ and $-\theta$ cancel the inductive voltage at resonance, the current in the wire at θ must be proportional to $\sin \theta$. This is the current distribution required to produce the assumed uniform field B_1 . The N segment birdcage may be thought of as $N/2$ such closed loops wired in parallel. Hence the net effective inductance of the cage is lower than a saddle coil with only two parallel turns. The more evenly distributed currents in the birdcage do not produce the high magnetic energy densities found near the conductors in the saddle coil. The nonuniform field near the edges of the saddle coil means less magnetic energy is stored inside the sample volume; hence, a saddle coil will have a poorer filling factor than a birdcage resonator. Likewise, the multiple parallel paths of the birdcage reduce the resistive losses compared to those of a saddle coil.

Using the Biot-Savart law, the rf field strength B_1 can be calculated for a saddle coil and birdcage resonator made from small diameter wire. Figure 3a shows a contour plot of rf field strength produced in the transverse midplane of a saddle coil. Figure 3b shows the analogous plot for a birdcage coil containing 16 wires. Figures 3c and d show images of a 240 mm diameter water phantom in a 270 mm diameter saddle coil and in a 285 mm diameter 16-wire birdcage resonator, respectively. The coils were oriented to produce a vertical B_1 field instead of the horizontal field computed in Figs. 3a and b. The smaller relative diameter of the saddle coil adds somewhat to the observed inhomogeneity. The alternating regions of high- and low-field strength extend into the sample volume for distances

comparable to the separation between the wires. Hence by increasing the number of conductors in the birdcage, the ripples in the field strength can be reduced nearly to zero. The number of wires is limited only by the need for the cylindrical surface to remain transparent to the rf flux.

The chief cause of B_1 inhomogeneity in the birdcage configuration is the unavoidable roll-off of field intensity at the ends of the coil. A long coil produces more uniform sensitivity for coronal and sagittal imaging. A short coil is more favorable for axial imaging because it picks up less noise from portions of the body outside the imaging plane. Hence a trade-off is required when choosing the coil length.

The SNR performance of the birdcage resonator is consistent with the treatment of imaging sensitivity by Hoult and Lauterbur (1). They considered three types of losses which could contribute noise, namely, the resistance of the coil, the magnetically induced eddy current losses in the sample, and the dielectric or conductive losses due to stray electric fields in the sample. Determining the individual contributions of the two sample loss mechanisms is not trivial. Putting a one gallon phantom filled with distilled water into a head coil tends to lower the resonant frequency without significantly lowering the coil quality factor Q . The high dielectric constant of water increases the effective stray capacitance. Adding about 0.2 wt% of NaCl to the phantom reduces the coil's Q approximately the same amount as a human head. The coil's resonant frequency is shifted less by the saline solution than the distilled water. We believe the magnetically induced sample currents reduce the effective inductance of the coil. The sample losses, however, could be due to rf electric or magnetic fields. In similar experiments with surface coils and lossy phantoms, we were able to vary the stray electric fields (as evidenced by the resonant frequency shifts) without varying the rf magnetic fields. No significant sample losses could be attributed to electric fields at 64 MHz in the surface coils. We assume that, from the frequency shifts observed in our head and body coils, electric-field-induced losses are small for these coils also. Hoult and Lauterbur pointed out that magnetically induced sample losses could (and should) become the dominant noise source for high-field clinical imaging. Their expression for the SNR for a spherical phantom of radius b with electrical conductivity σ is

$$\text{SNR} \propto \frac{\omega^2 B_1}{\sqrt{r_{\text{coil}} + r_{\text{sample}}}} \propto \frac{\omega^2 B_1}{\sqrt{\alpha\omega^{1/2} + \beta\sigma\omega^2 B_1^2 b^5}} \quad [2]$$

where B_1 is the rf field produced by the coil per unit current. The two terms in the denominator are proportional to two resistors: the first, r_{coil} , is the coil resistance with a frequency dependence due to the skin effect; the second, r_{sample} , is an equivalent series resistor due to the induced eddy current losses in the conductive sample. The sample losses increase rapidly with frequency and sample size. We have produced coils in which sample losses have significantly exceeded coil losses for fields above 0.3 T. In the high-field limit, where $r_{\text{sample}} \gg r_{\text{coil}}$, Eq. [2] reduces to

$$\text{SNR} \propto \frac{\omega}{b^{5/2}}. \quad [3]$$

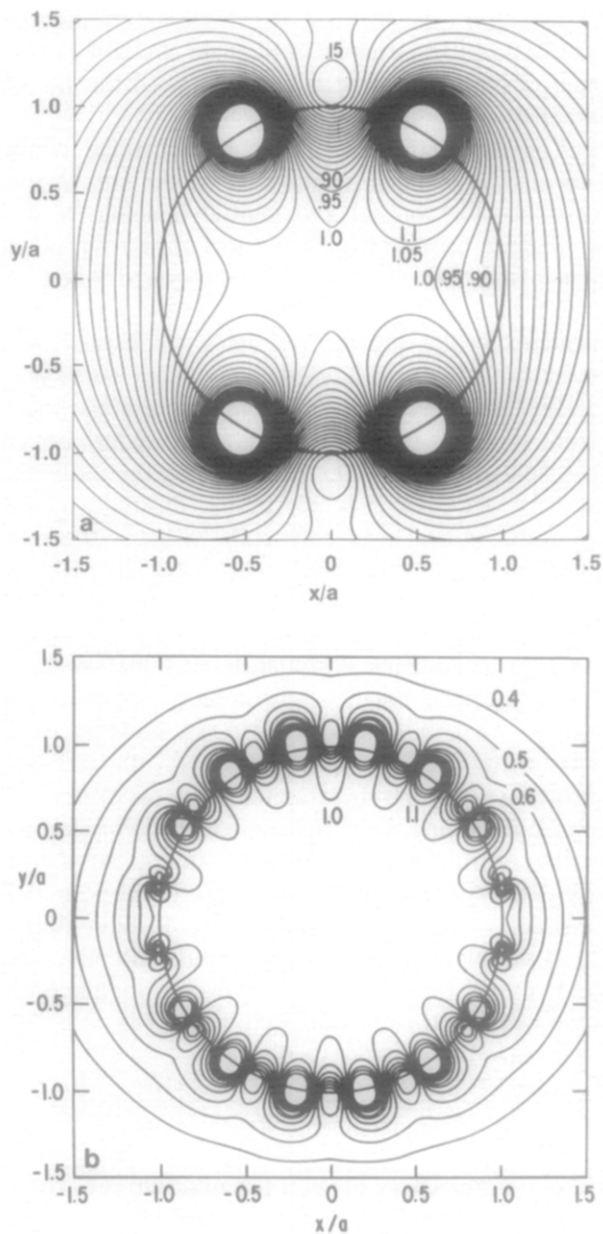


FIG. 3. Computed contour plots of constant rf field magnitude for the transverse midplane of a saddle coil (a) and a birdcage resonator (b). Images of a 240 mm diameter water-filled phantom in a saddle coil (c) and a birdcage resonator (d).

Note that the parameter B_1 , which depends on coil geometry, has dropped out. Hence, the difference in value for B_1 in solenoids and saddle coils, as described by Hoult and Richards (3), is unimportant for high-field imaging. Also note that SNR,

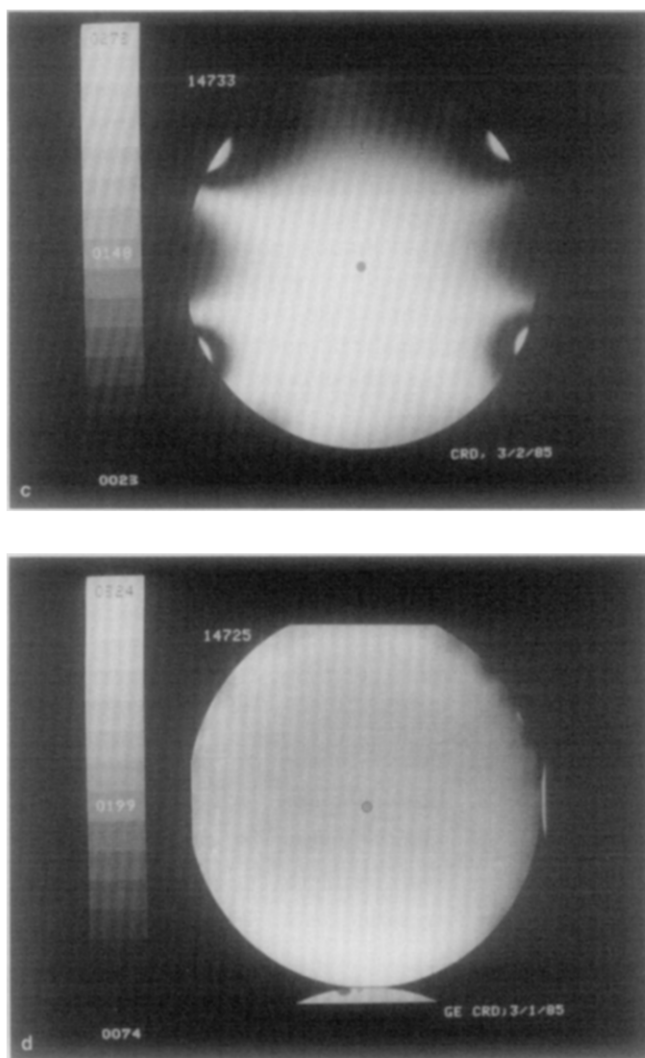


FIG. 3—Continued.

which refers to a fixed voxel size, decreases as the volume of lossy sample material increases.

The relative values of r_{coil} and r_{sample} can be determined by measuring the coil quality factor, Q , when the coil is empty and when it is loaded by the patient. The best indicator of coil sensitivity is the ratio

$$\frac{Q_{\text{empty}}}{Q_{\text{loaded}}} = \frac{r_{\text{coil}} + r_{\text{sample}}}{r_{\text{coil}}} \quad [4]$$

provided electric field losses do not contribute to r_{sample} . For our coils, this ratio is typically greater than five. This implies that the rf coil losses contribute less than 11% of the observed noise voltage. Hence further increases in empty coil Q or B_1

will have diminishingly small effects on the signal-to-noise ratio. Roeschman (5) indicates his Q ratio ranged from 2 to 3.3.

When the birdcage coil is constructed with fourfold symmetry, the desired homogeneous resonance will be doubly degenerate. The two modes are spatially and electrically orthogonal. Quadrature excitation of the two modes with currents of equal magnitude but with phases differing by 90° produces a circularly polarized rf field. The power required for a given nuclear flip angle with a circularly polarized field is one-half that required with a linearly polarized field (2). Similarly, each of the two orthogonal modes can be used to receive the resulting nuclear signal and accompanying noise voltage. Combining the two channels after one has been phase shifted 90° doubles the signal voltage. The noise voltage increases only by a factor of $\sqrt{2}$ because the two noise voltages are not correlated. Hence, quadrature reception enhances the SNR by a factor of $\sqrt{2}$.

When imaging large volumes of conductive medium at high fields with linear excitation and reception, rf field penetration effects tend to produce regions of enhanced and diminished signal strength as a function of θ . With quadrature excitation and reception, the dependence is averaged out to give a more uniform signal sensitivity. These effects have been discussed elsewhere (7).

REFERENCES

1. D. I. HOULT AND P. C. LAUTERBUR, *J. Magn. Reson.* **34**, 425 (1979).
2. C.-N. CHEN, D. I. HOULT, AND V. J. SANK, *J. Magn. Reson.* **54**, 324 (1983).
3. D. I. HOULT AND R. E. RICHARDS, *J. Magn. Reson.* **24**, 71 (1976).
4. W. S. HINSHAW AND R. C. GAUSS, U.S. Patent No. 4,439,733 (1984).
5. P. ROESCHMAN, Third Annual Meeting of the Society of Magnetic Resonance in Medicine, New York, New York, August 17-23, 1984, p. 634.
6. L. BRILLOUIN "Wave Propagation in Periodic Structures," p. 38ff, Dover, New York, 1946.
7. G. H. GLOVER, C. E. HAYES, W. A. EDELSTEIN, O. M. MUELLER, H. R. HART, C. J. HARDY, M. O'DONNELL, AND W. D. BARBER, Third Annual Meeting of the Society of Magnetic Resonance in Medicine, New York, New York, August 17-23, 1984, p. 264.